

# Fixed-Exit Monochromators for High-Energy Synchrotron Radiation

P. Suortti and C. Schulze

*European Synchrotron Radiation Facility, BP 220, F-38043 Grenoble CEDEX, France*

(Received 17 June 1994; accepted 22 August 1994)

Current developments in X-ray optics for synchrotron radiation beamlines are briefly reviewed. Reference is made to recent work on adaptive mirrors, cryogenic cooling of monochromators, use of thin diamond crystals, and active correction of the crystal shape for distortions caused by beam heating. The use of bent Si crystals as monochromators is discussed in detail. At high energies, Si crystals become transparent to X-rays allowing new monochromator constructions. Bending of the crystal increases the energy bandpass and allows focusing. Different combinations of bent crystals that provide a fixed exit beam are discussed. These include vertically diffracting meridionally focusing Laue–Laue crystals, a Laue crystal combined with a sagittally focusing Bragg crystal, and a Laue–Bragg pair of crystals which provides meridional focusing at two stages.

**Keywords:** high-energy monochromators; fixed-exit monochromators; Laue–Bragg monochromator; Laue–Laue monochromator.

## 1. Introduction

The X-ray optical solutions for crystallography beamlines have become rather standard in the last 5 or 10 years. Most of the modern designs are based on modular solutions, where wavelength tuning by a two-crystal monochromator and focusing by mirrors are separated. These instruments perform best in the traditional range of wavelengths for X-ray diffraction, *i.e.* around 1 Å or 10 keV in the energy scale. However, there are new developments and requirements that have changed this rather stabilized situation. First, tunable undulators of high-energy storage rings reach the 10 keV regime and provide superior brilliance. Second, there is a zest for higher energies, which can be reached only by high-power wigglers. These bring about new problems owing to the large thermal load and difficulties of conserving the brilliance of the source. Ingenious solutions have been introduced, and these will be reviewed briefly, but at energies of the order of 100 keV entirely new concepts of focusing and monochromatizing are needed.

The design of an X-ray optical system is always based on some kind of ray tracing. Ideally, for each individual ray, the change of direction, displacement from the center line, attenuation and polarization should be followed through the optical system. This becomes cumbersome, and in standard treatments the roles of various optical elements are not clear. In particular, the effects of beam penetration into the optical components and mixing of vertical and horizontal focusing are difficult to follow. A graphical method called phase-space analysis treats the optical components as windows in position–momentum–wavelength space, and the effect of each window is easy to separate (Matsushita & Hashizume, 1983; Suortti & Freund, 1989). When an appropriate X-ray optical solution has been found, it can be optimized by a detailed ray-tracing calculation.

## 2. Present X-ray optical components

Third-generation synchrotron sources have posed new challenges, as the X-ray optics should conserve the unprecedented brilliance. The quality of optical components must match that of the source under the heat load of the synchrotron beam. The vertical emittance of the electron beam at the ESRF is smaller than  $10^{-9}$  m rad, so that the geometrical tolerances of the mirrors and monochromators are in the  $\mu\text{rad}$  regime. Thermal distortions far exceed this limit unless new types of adaptive or inherently stable methods for cooling and control of geometrical shape are introduced.

Adaptive mirrors have been developed at the ESRF for wiggler beamlines, where the total power of the synchrotron radiation beam is up to 15 kW. The mirror is the first optical component, and it is bent vertically to parabolic shape to reduce the divergence of the incident beam. The actual profile of the mirror is measured on-line by a Schack–Hartmann interferometer, and the shape is corrected by piezo-crystal actuators attached to the back of the mirror. The precision of the final curvature, as measured in a test bench, is of the order of 1  $\mu\text{rad}$ . There are many difficulties under the actual beamline conditions, where the structures are deformed due to heating by scattered radiation, and where the optical parts may suffer radiation damage. However, commissioning of the adaptive mirror at the Materials Science Beamline has been largely successful, and is approaching routine operation (Susini, Krumrey, Baker & Kvick, 1994).

Cryogenic cooling of silicon monochromators was demonstrated a few years ago (Marot, Rossat, Freund, Joksch, Kawata, Zhang, Ziegler, Berman, Chapman, Hastings & Iarocci, 1992). The thermal expansion coefficient of Si approaches zero around 100 K, and, at the same time, the heat conductivity increases. The first crystal of the mono-

chromator is attached by an In–Ga eutectic to copper blocks that are cooled by liquid nitrogen. The method is in use at some of the undulator beamlines of the ESRF, and the first tests at a high-power wiggler beamline indicate that sufficient heat transfer is achieved by liquid nitrogen. Technical problems arise mostly from vibrations in the cooling circuit.

High-quality artificial diamond crystals of sufficient size have become available in recent years. These are ideal monochromators for synchrotron beams from undulator sources. Absorption is low and heat conduction high, so that the thermal distortion is small. Edge-cooled crystals in transmission geometry let most of the beam through the monochromators, allowing subsequent use of the beam. The so-called Troika beamline at the ESRF is based on this concept (Freund, 1993; Grüberl, Als-Nielsen & Freund, 1994).

Active crystal optics have been introduced by Quintana, Hart, Bilderback, Henderson, Richter, Setterston, White, Hausermann, Krumrey & Schulte-Schrepping (1995). In these monochromators, efficient water cooling is combined with correction for the thermal distortions by bending forces arising from the water pressure. These devices work in reflection geometry, and they have been constructed for the line geometry of an extended wiggler beam and for the essentially axial geometry of an undulator beam. Both silicon and diamond crystals have been used.

### 3. Bent silicon crystals at high energies

Attenuation and transmission of X-rays in silicon is shown in Fig. 1. The important feature is that below 100 keV the energy absorption coefficient decreases approximately as  $E^{-3}$  and is constant above that energy. The steep slope is due to photoelectric absorption and the constant part arises from the energy loss of the Compton recoil electrons. The

total attenuation coefficient is much larger at high energies, but the Compton quantum carries most of the energy. As to possible monochromator constructions, this has many important aspects. First, if the low-energy part of the spectrum is removed by filters, the energy absorbed in the crystal is small; in the case of Fig. 1 only 2% of the power above 100 keV is absorbed. Compton-scattered radiation leaves the crystal and is absorbed elsewhere causing thermal distortions of mechanical structures, unless shielding is used. Most of the direct beam passes through the crystal, so that it can be used subsequently at other monochromators or white-beam stations. The monochromators described below are constructed in such a way that the direct beam hits the Si crystal only, but not the cooled support.

Another important feature is that at high X-ray energies the extinction length increases in proportion to energy. The intrinsic angular widths of the reflections decrease, but on the other hand, any distortion of the crystal makes it diffract kinematically rather than dynamically. This fact can be utilized in cases where the highest resolution is not needed, but flux is important. Bending of the crystal in the meridional plane introduces an easily controllable distortion and provides focusing at the same time. Several constructions have been put forward, most notably in transvenous coronary angiography where bent Laue-type (transmission) monochromators have provided superior flux and focusing properties (Suortti, Thominson, Chapman, Gmür, Siddons & Schulze, 1993). These crystals have been thoroughly tested, and the experimental results agree closely with theoretical calculations, as shown in Fig. 2 (Schulze & Chapman, 1994). This gives confidence that theoretical evaluations of X-ray optical designs involving meridionally bent crystals can be made reliably.

At first sight, cooling of bent crystals seems to be difficult. However, efficient side-cooling schemes have been developed. In the case of the vertically focusing Laue crys-

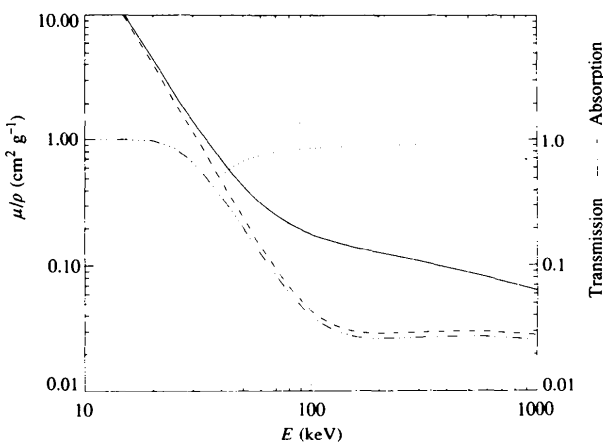


**Figure 1**

Attenuation and transmission of a 4 mm thick Si crystal. The total attenuation coefficient is given by the solid line and the energy absorption coefficient (Hubbell, 1982) by the dashed line. Energy absorption is given by the dot-dashed line and transmission of radiation by the dotted line.

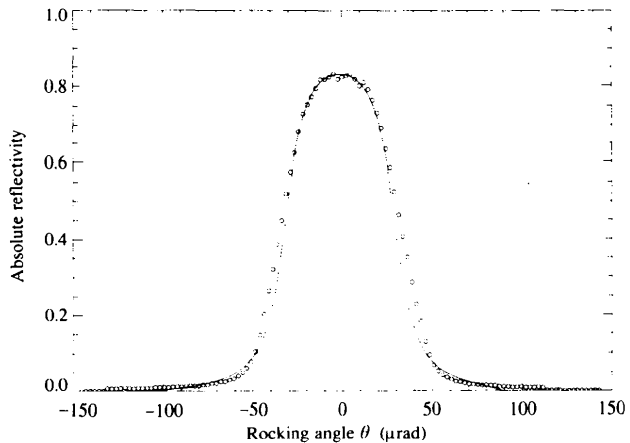


**Figure 2**

Measured (circles) and calculated (solid line) reflectivity curves of the 111 reflection for a cylindrically bent Laue-type Si-crystal monochromator. The thickness of the crystal is 0.7 mm, the asymmetry angle 26.22°, bending radius 12.97 mm, and the X-ray energy 33.17 keV.

tal for angiography, the Si crystal has a thin horizontal section in the middle, and cooling tubes are attached to the thick upper and lower edges of the crystal. The thin part is bent to cylindrical shape, and the thick edges provide rigidity. For horizontal focusing either in Laue or Bragg (reflection) geometry the crystal can be attached by the edges to a cooled frame, which is bent. An extensive study of thermal and mechanical distortions of crystal benders was made using finite-element analysis. Particularly in the Bragg case, where the angle of incidence is small and the crystal long, the calculation becomes essentially two dimensional. In a typical case, the temperature of the bender was found to change by less than 3 K over its length. This gradient introduces a bending radius larger than 20 km, which can be neglected. The shape of the crystal is determined by the bender frame, which is bent to a cylinder by two opposite moments. These can be produced in many different ways, and practical designs have been reviewed recently (Siddons, 1994). In all cases, it is important that force actuators are used instead of displacement actuators, because thermal expansion of the support structures may far exceed the displacement of the actuator. Prototypes have been used under beamline conditions with good results (Suortti, Lienert & Schulze, 1994).

#### 4. Bent two-crystal monochromators

##### 4.1. Laue–Laue combination

A non-dispersive pair of crystals can be realized in many different ways, the only requirement being that the exit beam of the first crystal matches the acceptance of the sec-

ond crystal in momentum space (Suortti & Freund, 1989). Even crystals that have different lattice spacings can be matched by appropriate choices of bending radii. In the following only a pair of crystals with the same lattice spacing is considered, because a fixed exit beam is required over a large energy range. Two possible Laue-type geometries are shown in Fig. 3. In both cases, the first crystal images the source to the source point for the second crystal. When the focus of the first crystal is a virtual source to the second crystal the exit beam diverges (Figs. 3a,b), but when the focus is a real source the exit beam converges (Fig. 3c). However, this simple geometrical picture is considerably complicated by diffraction in crystals of finite thicknesses. This is understood by considering a narrow polychromatic beam traversing a crystal of changing lattice spacing and orientation. A band of wavelengths is reflected, and at the exit surface a broadened but focused beam emerges. The polychromatic focus may be real or virtual, and usually it does not coincide with the geometrical focus. Accordingly, matching the two crystals includes making the polychromatic foci coincide. It should be noted that in the case of symmetrical Laue reflection from a bent crystal the change of lattice-plane orientation exactly compensates the effect of the change of lattice spacing across the crystal, so that there is no wavelength dispersion, and this has been utilized in high-resolution  $\gamma$ -spectrometers (Börner, 1990).

One of the above combinations of Laue-type crystals has been studied in detail (Schulze, Suortti & Chapman, 1994). The aim of the study was to develop a fixed-exit tunable monochromator for computed tomography (CT). Earlier attempts with two flat crystals have largely been failures

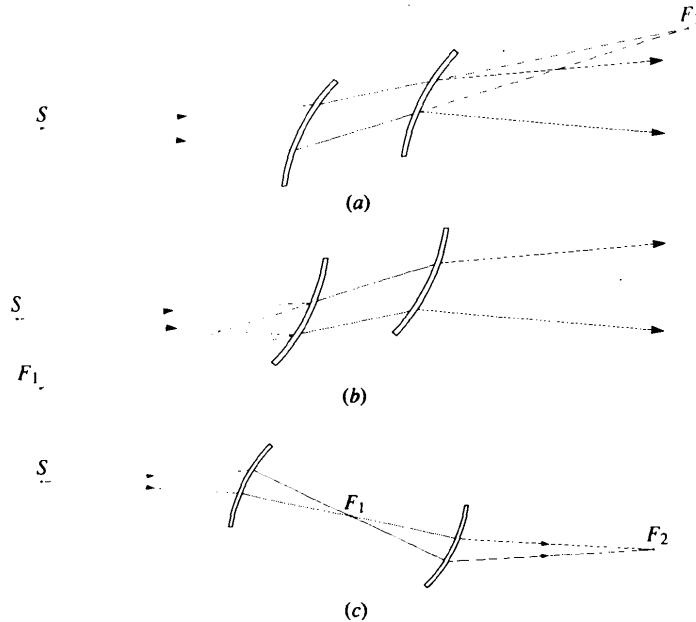


**Figure 3**

Non-dispersive settings of two Laue-type crystals. In each case, the focus of the first crystal is the source point for the second crystal: (a) corresponds to polychromatic and (b) to monochromatic focusing, where the source for the second crystal is virtual, and the exit beam diverges. In the polychromatic case (c), the source for the second crystal is real, and the exit beam then converges.

because of the difficulty of matching the rocking curves of perfect crystals at high energies for beam widths larger than 20 cm. The rocking curve widths decrease in proportion to the X-ray wavelength, and a thin flat crystal is inherently unstable. Bending of the crystal both increases the width of the rocking curve and stabilizes the shape. Fig. 4 shows the increase of the width of a reflection when the bending radius is decreased. A prototype monochromator was constructed utilizing the combination shown in Figs. 3(a) and 3(b). Test measurements were made both in the broad-band mode, where the beam enters from the convex side of the crystals, and in the monochromatic mode where the source is on the focusing (Rowland) circle. The reflectivity curve of the monochromator was analyzed by a perfect flat crystal. A scan across the monochromator face showed that the reflectivity stayed constant and the shift followed the change in the angle of incidence, proving that the crystals were uniformly bent to cylinders, which had parallel axes. In practice, there are numerous possibilities for matching the crystals, as the bending radii, asymmetric cuts and thicknesses of the crystals can be varied independently, but in the optimum situation the geometrical foci of the two crystals coincide and the reflectivity curves have equal widths. The output flux of such a monochromator is enhanced by an order of magnitude over a pair of flat crystals, and the beam is uniform and stable. The bandpass for each individual ray is increased, but the total bandpass may be reduced when the source is placed on the focusing circle. This inverse Cauchois geometry reduced the bandpass by a factor of 4 in the present case.

#### 4.2. Laue–Bragg combination

The Laue–Bragg combination of two flat crystals is a well-known construction for a fixed-exit monochromator (Mills, 1983). However, when the crystals are bent many new possibilities appear. One of the standard constructions

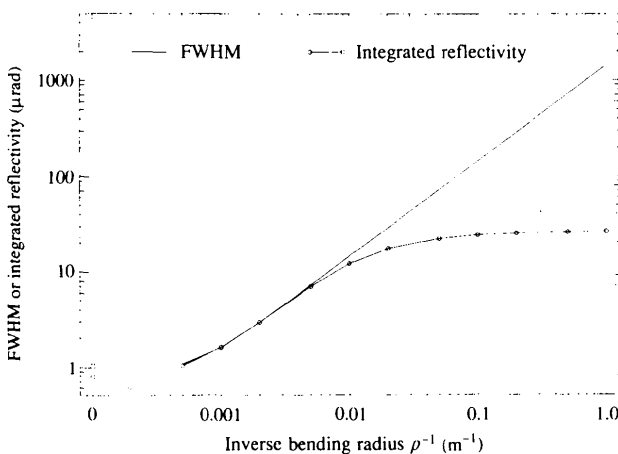


**Figure 4**  
Calculated width and integrated reflectivity of the 422 reflection from a cylindrically bent Si crystal as a function of the inverse bending radius. The thickness of the crystal is 1 mm, the asymmetry angle 35.26° and the X-ray energy 75 keV.

of two-crystal monochromators is a pair where the first crystal is flat and the second is bent sagittally for horizontal focusing. The second crystal should be of cylindrical shape to maintain the non-dispersive setting of the two crystals, but unless constrained, the sagittally bent crystal assumes a saddle shape (anticlastic bending). The constraints that are used are stiff longitudinal ribs or edges, but the crystal becomes segmented, and the difficulty of matching the crystals increases with the photon energy. The main problem is that the construction does not allow any fine tuning of the crystals in the meridional plane. This may be avoided by a Laue–Bragg pair of crystals, where the meridional curvature due to the anticlastic bending of the second crystal is compensated by bending the first crystal, as illustrated in Fig. 5. The Laue–Bragg pair is vertically focusing, and the divergence of the exit beam is equal to that of the incident beam,  $\psi_1 = h/F_1$ , where  $h$  is the height of the slit and  $F_1$  the distance from the source. The crystals form a non-dispersive pair, when the divergence of the beam from the first crystal is

$$\psi_2 = \psi_1 + \varphi = h/F_1 + h/R_a \sin\theta, \quad (1)$$

where  $R_a$  is the anticlastic bending radius and  $\theta$  the Bragg angle. This is related to the sagittal radius  $R_s$  by  $R_a = R_s/Cv$ , where  $v$  is the Poisson ratio and  $C$  a constant that takes account of the constraints arising from clamping of the crystal. In the case of a narrow long crystal,  $C$  approaches zero, but a typical value may be  $C = 0.2$ . In the symmetrical case  $R_s = F_1 \sin\theta$ , and the focal length of the Laue crystal is

$$F_2 = -h/\psi_2 = -F_1(1 + Cv/\sin^2\theta)^{-1}. \quad (2)$$

The bending radius is

$$\rho = 2F_1F_2 \cos\theta/(F_1 + F_2) \quad (3)$$

and the energy bandpass

$$\Delta E/E = \cot\theta h(F_1 - F_2)/2F_1F_2. \quad (4)$$

The signs are chosen such that  $F_1$  is positive,  $F_2$  is positive when on the same side of the crystal as  $F_1$ , and  $\rho$  is positive when the incident beam is on the concave side (Suortti, 1992). Some values are collected in Table 1, assuming  $Cv = 0.04$ . The energy bandpass is larger than for a flat-crystal monochromator, but this may be tolerable in many applications. So far, this idea has not been implemented,

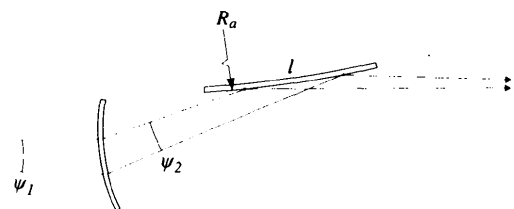
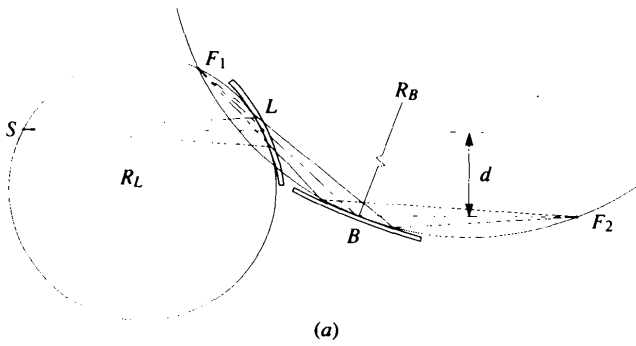
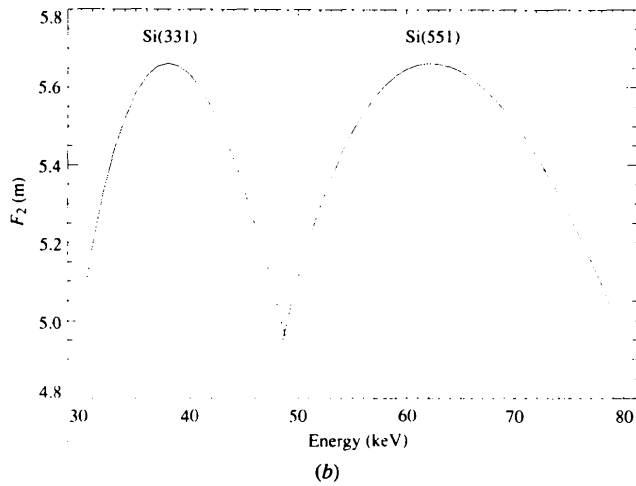


**Figure 5**  
Non-dispersive pair consisting of a bent Laue crystal and a sagittally focusing anticlastically bent Bragg crystal.



(a)



(b)

**Figure 6**

Meridionally bent Laue–Bragg crystal combination for horizontal focusing. The geometrical arrangement, where the Rowland circles of the crystals cross at  $F_1$ , is shown in (a). The focal distance of the monochromator,  $F_2$  is shown in (b) for two pairs of crystals. The parameters of the monochromator are collected in Table 2.

**Table 1**

Parameters of a monochromator where a bent Laue crystal is used to compensate for the anticlastic bending of the sagittally focusing Bragg crystal.

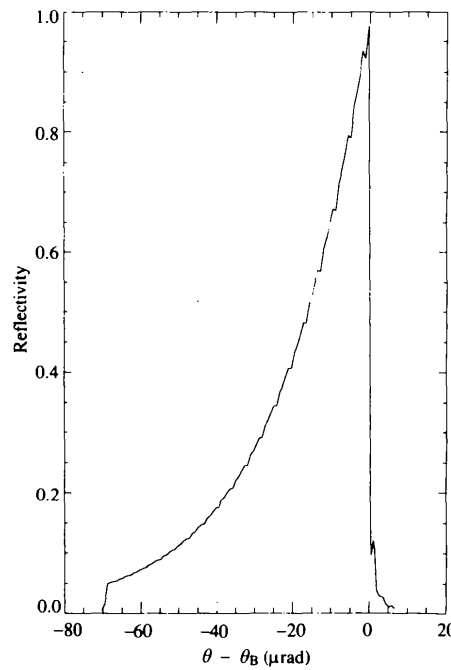
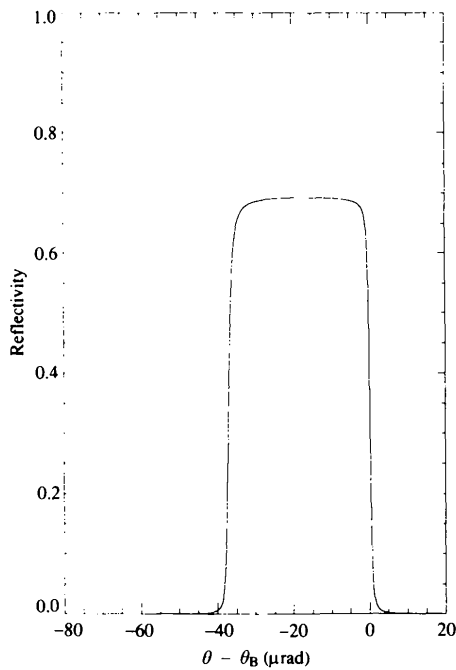
$E$ (keV)	$\sin\theta$	$R_s$ (m)	$R_a$ (m)	$F_2$ (m)	$(\Delta E/E)$	$(\Delta E/E)_o$
30	0.1522	4.57	114.2	-11.0	$1.2 \times 10^{-3}$	$0.65 \times 10^{-3}$
40	0.1142	3.43	85.7	-7.4	$2.2 \times 10^{-3}$	$0.87 \times 10^{-3}$
50	0.0913	2.74	68.5	-5.2	$3.7 \times 10^{-3}$	$1.10 \times 10^{-3}$

Notes: The distance from the source is 30 m, the slit height is 3 mm, and the ratio  $C_V$  between the sagittal and anticlastic radii is taken as 0.04. An Si(400) crystal was used. The energy resolution is given for this combination, and for flat crystals for comparison [subscript (o)].

but a similar compensation of anticlastic bending and the thermal ‘bump’ of the first crystal in the Bragg–Bragg pair has been inferred (Zontone & Comin, 1992).

It has been demonstrated above that various types of meridional focusing can be achieved by bent crystals in Laue and Bragg geometries. It is obvious on geometrical grounds that a tunable fixed-exit Laue–Bragg or Bragg–Laue monochromator can be constructed, but it turns out that with suitable choices of the focal lengths the focus is also practically fixed for large energy ranges. The X-ray source is on the Rowland circle of the first crystal, and the image is on that of the second crystal, so that monochromatic focusing is achieved in two stages. One example is shown in Fig. 6, where pairs of Si(331) and Si(551) crystals cover energies from 30 to 80 keV, and the focal length is constant within 10%.

The broadening of the reflectivity curves due to the effective thickness of the crystals offers many possibilities of matching and fine tuning of the crystal pair. The reflec-

**Figure 7**

Reflectivity curves of the Si(331) crystals in the arrangement shown in Fig. 6; Laue crystal to left, Bragg crystal to right.

tivity curves of a crystal pair are shown in Fig. 7. When the curves are superimposed it is obvious that the crystals are much easier to match than a pair of two flat crystals, as already demonstrated in the Laue-Laue case. The integrated reflectivity is increased by an order of magnitude due to a similar increase in the bandpass, which is still well suited for diffraction studies. However, it has already been noted that the energy dispersion across the reflectivity curve is accompanied by displacement and focusing of each beam element. In a simplified geometrical interpretation (Suortti *et al.*, 1994), the polychromatic beam reflected from the incident beam has a finite width at the crystal exit surface,

$$w = T \sin 2\theta / \cos(\chi + \theta), \quad (5)$$

where  $T$  is the thickness of the crystal, and  $\chi$  the angle between the Bragg planes and the surface normal of the crystal. The divergence of the beam is twice the width of the reflectivity curve. This picture is modified by the actual propagation of the wavefields inside the crystal and the boundary conditions at the exit surface. However, in the same way as in the Laue-Laue combination, at least a part of the reflected beam will find suitably oriented lattice planes in the second crystal, as illustrated in Fig. 8. The bending radii of the crystals are almost equal, and the widths of the reflectivity curves are comparable yielding maximum flux. A comparison with a vertically reflecting flat crystal monochromator is revealing. The energy bandpass of the present monochromator is close to the Darwin width of Si(111), while at high energies the resolution of a flat-crystal monochromator is dominated by the vertical divergences of the beam. At the same time, the bent-crystal monochromator provides six times more flux than a pair of flat crystals.

Design parameters of a Laue-Bragg bent-crystal monochromator are collected in Table 2. The Laue crystal is placed first for practical reasons. The length of the crystal is rather small, and an effectively cooled crystal bender is

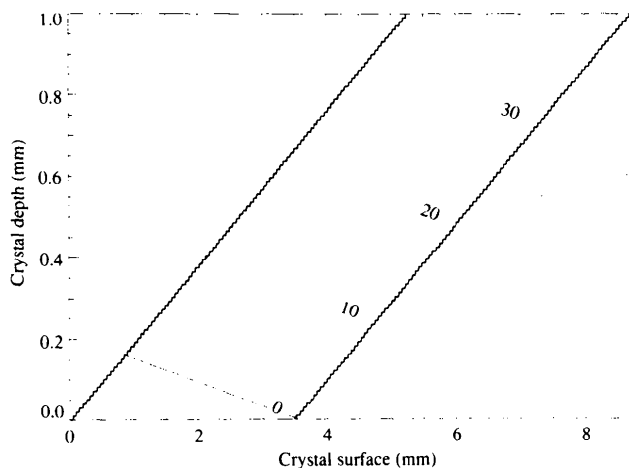


**Figure 8**

Successive reflections of a narrow beam from meridionally bent Laue and Bragg crystals. The numerical values correspond to an Si(331) pair of crystals as specified in Table 2. The beam inside the Bragg crystal is indicated by thick lines. The thin line shows where the beam is reflected. When the Laue crystal is rotated to larger angles this line moves deeper in the Bragg crystal, as indicated by the dotted lines, which correspond to energy shifts of multiples of  $-10$  eV.

**Table 2**

Parameters of a meridionally focusing Laue-Bragg monochromator.

			Crystal pair	
	Laue	Bragg	331/331	551/551
Source distance (m)	40			
Lateral displacement $d$ (cm)		10		
Asymmetry angle ( $^\circ$ )	74.5	3.6		
Thickness (mm)	1	1		
Bending radius (m)	104	80		
$(\Delta E/E)_{L-B}$			$3.0 \times 10^{-4}$	$3.0 \times 10^{-4}$
$(\Delta E/E)_o$			$8.0 \times 10^{-4}$	$8.0 \times 10^{-4}$
$P_{L-B}$			$12.6 \times 10^{-6}$	$2.4 \times 10^{-6}$
$P_o$			$2.2 \times 10^{-6}$	$0.4 \times 10^{-6}$

Notes: The crystal pairs are Si(331) and Si(551), and the values correspond to energies of 40 keV and 65 keV, respectively. The meridionally focusing Laue-Bragg crystal monochromator is indicated by subscript (L-B) and that of vertically reflecting flat crystals by subscript (o). The relative bandpass and integrated reflectivity  $P$  are given for each case.

easily constructed. The beam falling on the Bragg crystal is demagnified by a factor of 2.2, so that this crystal is also rather short, and there is no need for cooling. The bending radii of the crystals are almost equal, and the widths of the reflectivity curves are comparable yielding maximum flux. A comparison with a vertically reflecting flat crystal monochromator is revealing. The energy bandpass of the present monochromator is close to the Darwin width of Si(111), while at high energies the resolution of a flat-crystal monochromator is dominated by the vertical divergences of the beam. At the same time, the bent-crystal monochromator provides six times more flux than a pair of flat crystals.

The performance of the components of bent-crystal Laue-Bragg monochromators has been demonstrated with several prototypes, including cooling under high heat loads. Construction of the monochromator is underway, and the results of testing will be published separately.

A design study of bent water-cooled monochromators was made at TNO Industrial Research (Holland) by the group of P. van Zuylen. The prototypes were designed by M. Kretzschmer at the ESRF and tested at the Materials Science Beamline. We thank the beamline staff for their assistance, particularly H. Graafsma and Å. Kvick.

## References

- Börner, H. (1990). Private communication.
- Freund, A. K. (1993). *ESRF Newslett.* **19**, 11–13.
- Grübel, G., Als-Nielsen, J. & Freund, A. K. (1994). *J. Phys. (Paris)*. In the press.
- Hubbell, J. H. (1982). *Int. J. Appl. Rad. Isot.* **33**, 1269–1290.
- Marot, G., Rossat, M., Freund, A. K., Joksch, S., Kawata, H., Zhang, C., Ziegler, E., Berman, L., Chapman, D., Hastings, J. B. & Iarocci, M. (1992). *Rev. Sci. Instrum.* **63**, 477–480.
- Matsushita, T. & Hashizume, H. (1983). *Handbook of Synchrotron Radiation*, Vol. 1, edited by E. E. Koch, ch. 1. Amsterdam: North Holland.
- Mills, D. M. (1983). *Nucl. Instrum. Methods*, **208**, 355–358.

- Quintana, J., Hart, M., Bilderback, D. H., Henderson, C., Richter, D., Setterston, T., White, J., Hausermann, D., Krumrey, M. & Schulte-Schrepping, H. (1995). *J. Synchrotron Rad.* **2**, 1–5.
- Schulze, C. & Chapman, D. (1994). *Rev. Sci. Instrum.* In the press.
- Schulze, C., Suortti, P. & Chapman, D. (1994). *Synchrotron Rad. News*, **7**(3), 8–11.
- Siddons, D. P. (1994). *Rev. Sci. Instrum.* In the press.
- Suortti, P. (1992). *Rev. Sci. Instrum.* **63**, 942–945.
- Suortti, P. & Freund, A. K. (1989). *Rev. Sci. Instrum.* **60**, 2579–2585.
- Suortti, P., Lienert, U. & Schulze, C. (1994). *Nucl. Instrum. Methods*, **A338**, 27–32.
- Suortti, P., Thomlinson, W., Chapman, D., Gmür, N., Siddons, P. & Schulze, C. (1993). *Nucl. Instrum. Methods*, **A336**, 304–309.
- Susini, J., Krumrey, M., Baker, R. & Kvick, Å. (1994). *Rev. Sci. Instrum.* In the press.
- Zontone, F. & Comin, F. (1992). *Rev. Sci. Instrum.* **63**, 501–504.